P2.104 TROPICAL CYCLONE FLOW STRUCTURE IN THE PRESENCE OF ELEVATED TERRAIN

Brian J. Billings*
National Research Council, Monterey, CA

James D. Doyle
Naval Research Laboratory, Monterey, CA

1. INTRODUCTION

Wu and Kuo (1999) identify the top three priorities of typhoon forecasts near Taiwan as 1) track forecasts, 2) intensity forecasts, and 3) wind and precipitation forecasts. They also note that understanding the influence of the island's complex terrain is crucial to generating accurate forecasts. In the succeeding ten years, there has been a large amount of research on track forecasts and an increasing emphasis on precipitation forecasts. However, the forecast of intensity and the surface wind field associated with a landfalling typhoon has received less attention, particularly the later case.

Fudeyasu et al. (2008) examine a downslope windstorm and mountain wave activity associated with the landfall of Typhoon Pabuk on Japan, while Ramsay and Leslie (2008) studied the wind field of severe Tropical Cyclone Larry as it made landfall on the northeastern coast of Australia. Both of these studies utilized real-data MM5 forecasts to aid in an interpretation of terrain effects. Real-data simulations of this nature have the advantage of more closely agreeing with observed events, but it is often difficult to extract fundamental relationships from the numerous other processes being represented by the model. For this purpose, an idealized modeling framework can be used to more directly control the variations in the hypothesized controling parameters.

This study uses idealized numerical simulations performed with the Naval Research Laboratory's Coupled Ocean-Atmosphere Mesoscale Prediction System (COAMPS®) to investigate the effect of an island mountain with similar dimensions to Taiwan on an idealized typhoon's track, structure, intensity, and ultimately on the surface wind field that results as the storm interacts with the topography. Of particular interest are regions of reduced wind speeds in close proximity to the typhoon and regions of increased wind speeds at locations far removed from the storm center.

2. MODEL SETUP

This study uses the same version of COAMPS used in real-time forecasting of tropical cyclones (COAMPS-TC, Reynolds et al. 2010); however, for simplicity, the moving nest option is not used. The computational domain is 1536 x 1536 km with 6 km horizontal resolution and 40 vertical levels stretching from 20 m resolution near the surface to $>$ 2 km near the model top. All of the normal model physics are used (including explicit moist physics in place of a cumulus parameterization) with the exception of the radiation scheme which is not applied.

The initial sounding profile is based on the Dunion and Marron (2008) mean tropical sounding for a non-Saharan air layer, which uses a lower tropospheric relative humidity of 57%. A constant sea surface temperature of 29°C is used through the entire domain. The terrain is based on the same elliptical, sinusoid island used by Yeh and Ellsberry (1993a,b) except the dimensions are more closely matched to those of Taiwan with a length of 325 km, a width of 125 km, and a maximum height of 3 km. The island is located approximately 450 km from the western boundary of the grid and its vertical position is varied in the sensitivty experiments. The idealized tropical cyclone is an axisymmetric Rankine vortex with a fixed radius and a variable maximum wind speed. The idealized vortex was tested for a simulation with no mean flow and was found to maintain symmetry throughout the simulation. This vortex is placed into a mean, easterly geostrophic flow which is constant across the domain and throughout the depth of the atmosphere. It is located approximately 375 km from the eastern boundary of the domain. This leaves about 675 km between the peak of the island and the eye of the tropical cyclone at initialization. When the simulation is run for ninety-six hours, this leaves sufficient time for the vortex to spin-up and pass over the island with some degree of separation.

3. CONTROL SIMULATIONS

Before we examine the results of the simulations with interaction between a tropical cyclone and a mountainous island, we should first observe the properties of these two situations (a tropical cyclone propagating in a mean flow and flow over an obstacle) in isolation. For this reason, two control simulations were performed with either the vortex or the island removed.

3.1 *Ocean Control*

In this simulation, the vortex was placed in the flow, but the island was not. The resulting track is shown in Fig. 1. While there are some small deviations to the north and south, the mean track remains nearly horizontal toward the east through ninety-six hours. This an advantage over previous studies with coarser resolution where

* *Corresponding author address:* Brian Billings, Naval Research Laboratory, 7 Grace Hopper Ave, Monterey, CA; e-mail: brian.billings@nrlmry.navy.mil

the ocean control runs already had a significant track deviation to the north or south. Since the ocean control is nearly straight, any deviations when the island is inserted can be attributed to terrain-induced effects.

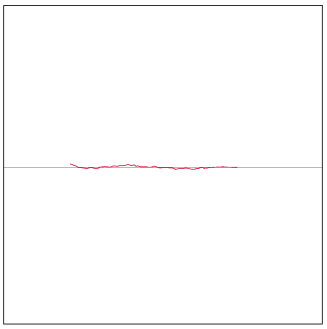

FIG. 1: Simulated track for ocean control simulation.

Many recent typhoons which have had a significant impact on Taiwan, such as Sinlaku and Jangmi in 2008, were characterized by maximum wind speeds of 50-60 m s^{-1} as they approached the island, which is much more intense than the storms simulated in many previous idealized studies. Figure 2 shows the maximum 10 m wind speed for the tropical cyclone in the ocean control simulation. Even though the Rankine vortex is defined with a maximum wind speed of 60 m s^{-1}, the storm has weakened nearly 30 m s^{-1} after two hours. There is continued weakening for the next twenty-four hours, after which the storm reintensifies at a more rapid rate so that the maximum wind speed reaches 45-50 m s^{-1} between thirty and thirty-six hours. After this time, the intensity continues to vary, but remains in the 50-60 m s^{-1} range mentioned earlier.

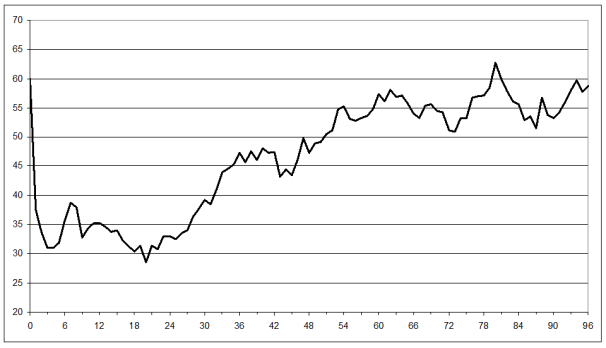

FIG. 2: Maximum 10 m wind speed for each hour of the ocean control simulation.

Figure 3 shows the surface wind field for the ocean control typhoon at the 72 h forecast time. The gale force winds extend out to a diameter of about 175 km, typical for a tropical cyclone. However, the weaker cyclonic circulation covers a much larger area, nearly filling the entire domain despite the mean easterly flow. This is appropriate for this study given that many typhoons impacting Taiwan contain circulations larger than the dimensions of the island. On the other hand, the eyewall is more compact than a typical typhoon with a diameter of approximately 50 km. This will likely have a significant effect for tracks passing near the ends of the island.

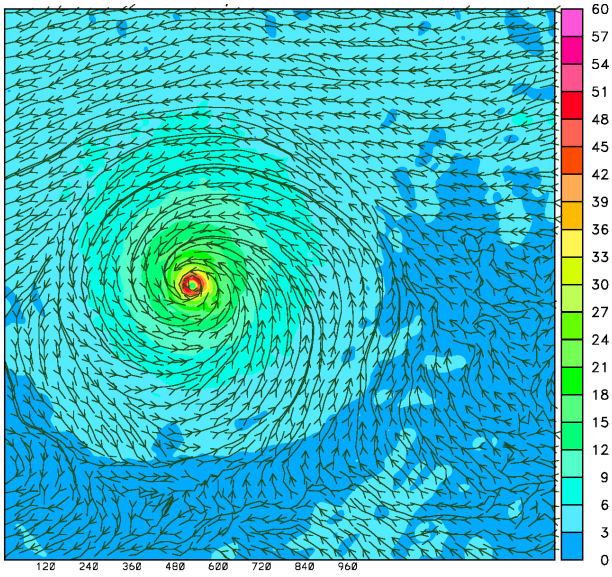

FIG. 3: 10 m streamlines and wind speed (shaded) for ocean control simulation.

3.2 *Terrain Control*

In this simulation, the island is placed within the mean flow, but the vortex is not inserted. As shown in Fig. 4, the flow in this situation is largely blocked with most of the air flowing around the island with deceleration upstream and acceleration around the edges. This is consistent with other studies of the flow associated with tall mountain islands (Smolarkiewicz and Rotunno 1989) and has been used to explain northward and southward track deflections depending on the location where the tropical cyclone approaches the island (Yeh and Elsberry 1993a).

With regards to the wind speed, there are only two regions of slightly stronger flow. To the north and south of the island, there are two areas of accelerated flow greater than the mean background flow, but still less than 6 m s^{-1}, where the air is forced around the terrain. Much of this increased flow is over ocean waters, but there are affected areas on the northeast and southeast coasts of the island. The northern vortex to the lee of the island also has an enhanced return flow; however, there are no areas of high surface winds in the presence of the mean

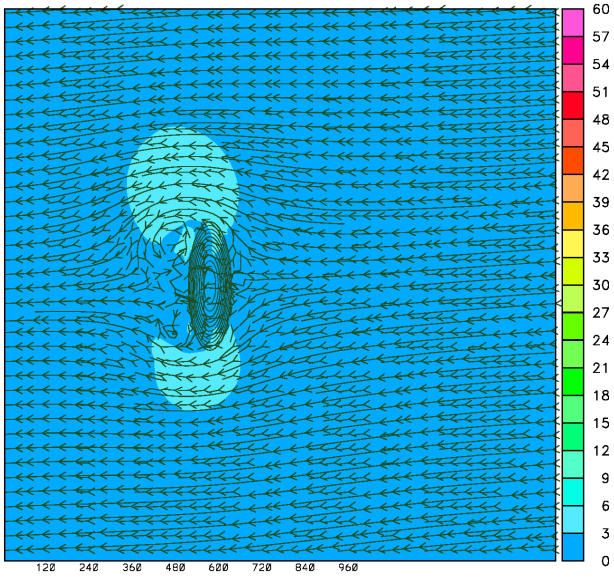

FIG. 4: Same as Fig. 3 for terrain control simulation.

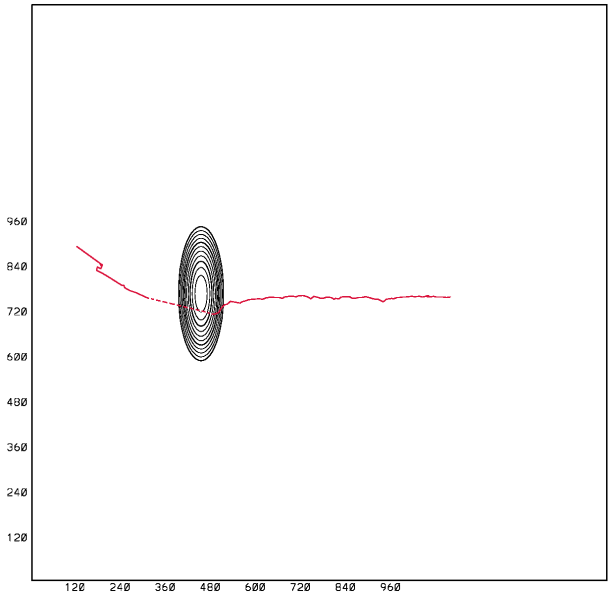

FIG. 5: Simulated track for the y=0 simulation. The dashed line represents where the track is discontinuous.

background flow.

4. TERRAIN-INDUCED TRACK DEFLECTIONS

Previous studies have shown that track deflection experienced by a tropical cyclone is sensitive to the relative positions of the vortex and the obstacle (Yeh and Elsberry 1993a). This is significant because actual typhoons can approach the Taiwan coast at a number of different locations. To maintain spacing between the vortex and the boundaries, each simulation initializes the storm along the domain's centerline and varies the vertical position of the island, resulting in a number of approach points from the south to the north end of the island.

Figure 5 shows the simulated track for a storm which is initially located on a direct line with the center of the island. No significant track deflections occur until the center of the storm circulation is about to make landfall. At this time, the tropical cyclone experiences a sharp southward deflection and continues moving along the upstream coast of the island while continuing to weaken and eventually dissipate. As the primary low begins moving southward, a secondary low forms along the northwest coast (Fig. 6). This low continues to strengthen and begins to move away from the island resulting in a discontinuous track when the primary low decays and the upper-level circulation continues over the island. Note that the COAMPS-TC automated tracking program is based on the center of the circulation and does not identify the secondary low immediately upon formation or maintain the primary low until its actual dissipation.

Figure 6 also shows the degree to which the storm is weakened as it makes landfall. Upstream of the island, the typhoon reaches a minimum central pressure of 946 hPa. At the time of landfall, the storm still has a central pressure of 979 hPa, but after this point, the eye rapidly fills to 990 hPa only four hours later. After an additional four hours, the original low is barely discernable, and a weak ($>$ 992 hPa) secondary low has started to move away from the island.

Figure 7 shows the simulated tracks from four additional model runs with the typhoon approaching $\pm$ 60 or 120 km from the center of the island. For the storms approaching the north end of the island, the resulting track is similar to the centered case with a southward defelction near the time of landfall and a secondary low forming and replacing (or in the northermost case, merging with) the primary storm. For the two simulations with the typhoon located to the south, the tracks are distinctly different. For the case with the typhoon located 60 km to the south, there is again a southward deflection, but it is much smoother and begins to occur much further upstream than for the northern cases. Also, while cyclonic vortices form to the lee of the mountain, there is not an associated pressure low and the upper-level circulation does not rephase with these circulations. Instead the storm continues to weaken off the southwestern coast. The case of a storm approaching the southern tip of the island results in much less deflection and landfall occurs in nearly the same location as for the storm initialized further to the north. Significant weakening again occurs as the storm is crossing over the island.

Lin et al. (2005) argue that northward track deflection will occur when the radius of a typhoon's maximum winds is much larger than the cross-flow length scale of the obstacle and that southward track deflection will occur when this radius is much smaller than the island. Given the small size of the simulated eyewall ($\sim$ 50 km in diam-

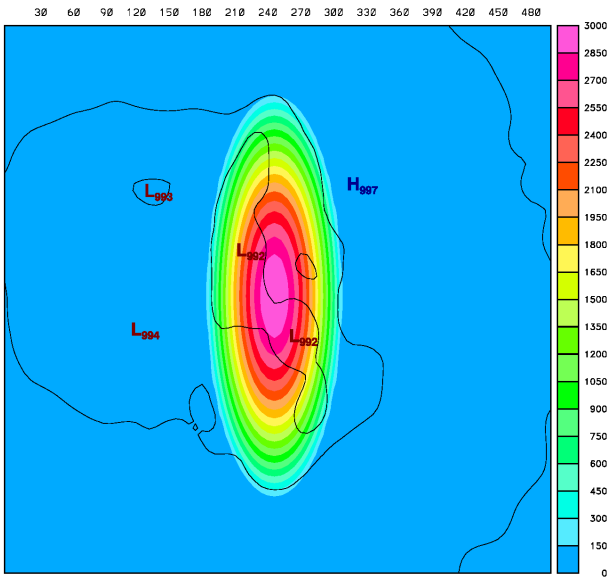

FIG. 6: Mean sea-level pressure at 75 hours integration for the y=0 simulation.

eter) and the large cross-valley with of the idealized island (325 km), the results of these simulations agree with the conclusions of Lin et al. (2005) since each storm experiences a southward deflection. Attempts were made to vary the size of the simulated storm by modified the model's turbulent subgrid scale mixing scheme. While this does expand the size of the eyewall, this comes at the cost of a significantly reduced intensity. Since the dimensions of the obstacle are easier to control in this idealized framework than the dimensions of the spun-up storm, additional simulation will be performed for a centered track and a reduced island length and width.

5. SURFACE WIND FIELDS

Figure 8 shows the surface wind fields from a time period near landfall for three simulations: one for a storm approaching the northern end of the island, one for a storm approaching the southern end, and one for a storm approaching the center of the island. A major feature of interest for the northern case is the large, low wind speed wake which forms along the southeastern coast. This region, which would be expected to contain a lower damage potential, extends northward far enough that winds less than 10 m s^{-1} are within 20 km of the typhoon eyewall, which is still producing winds of 30-35 m s^{-1} (60-65 kts). (Recall that the mean flow prescribed for this case is 2.5 m s^{-1}).

The typhoon in the southern landfall case also exhibits a slightly asymmetric wind structure, but due to different physical processes. First, the storm appears to have merged with a tip jet which formed in the westerly flow around the southern end of the island. One can note the similarity in wind speeds, placement, and orientation between the winds on the south end of the typhoon and the undisturbed tip jet in the easterly flow around the north end of the island. In addition to this elongation of higher winds to the south of the eye, there is a low-wind area to the north due to blocking effects on the upstream side of the mountain range. At the stagnation point, wind speeds are less than 3 m s^{-1} and are less than 12 m s^{-1} over a wider area. As with the wake in the northern landfall case, this particular area would be expected to experience relatively less wind damage at this particular time.

Another feature of interest in the southern landfalling case is the strip of higher wind speeds ($>$ 18 m s^{-1}) to the north of the typhoon along the island's lee slopes. This downslope flow separates before reaching the bottom of the mountain, resulting in a much weaker winds along the coastline. Figure 9 shows a vertical cross-section of the zonal wind speed and potential temperature through this downslope flow. A vertically propagating wave with slight downstream advection has developed just to the lee of the mountain. The wave at lower levels has steepened to very near the point of overturning, though there are no reversed zonal winds at this time period. Strong winds of nearly 25 m s^{-1} are being channeled between this level and the surface in a similar manner to that shown by Clark and Peltier (1977). This flow structure is not surprising due to the large amplitude of the mountain barrier and the mean flow being constant in height. For the case, where the typhoon makes landfall near the center of the island, all three of the previously discussed features are present, although they are reduced in magnitude compared to the landfalls on the north and south end of the island.

6. SUMMARY

This study has used idealized COAMPS-TC simulations to study the interaction of an intense tropical cyclone with a tall, elliptical island mountain for a variety of initial landfall points. For the cases where the storm approached the center or northern regions of the island, there was a significant southward deflection along the coastline and secondary low formation to the northwest with a resultant discontinuous track. When the storms approached the southern portion of the island, there was still a southward deflection, but it occurred further upstream and was smaller in magnitude. Additionally, in these southern cases, the upper-level low did not phase with any secondary lows and the track was a continuous one. In all simulations, the initial vortex weakened very rapidly after making landfall.

The presence of the elevated terrain resulted in regions of higher and lower wind speeds which would not be expected based on their distance from the eye of the tropical cyclone. Weaker wind regions formed for northern landfalling storms in a leeside wake to the south of the eye and for southern landfalling storms in blocked upslope flow to the north of the eye. Stronger wind regions formed in tip jets on either side of the island for both cases and in downslope flow on the northern half of the island

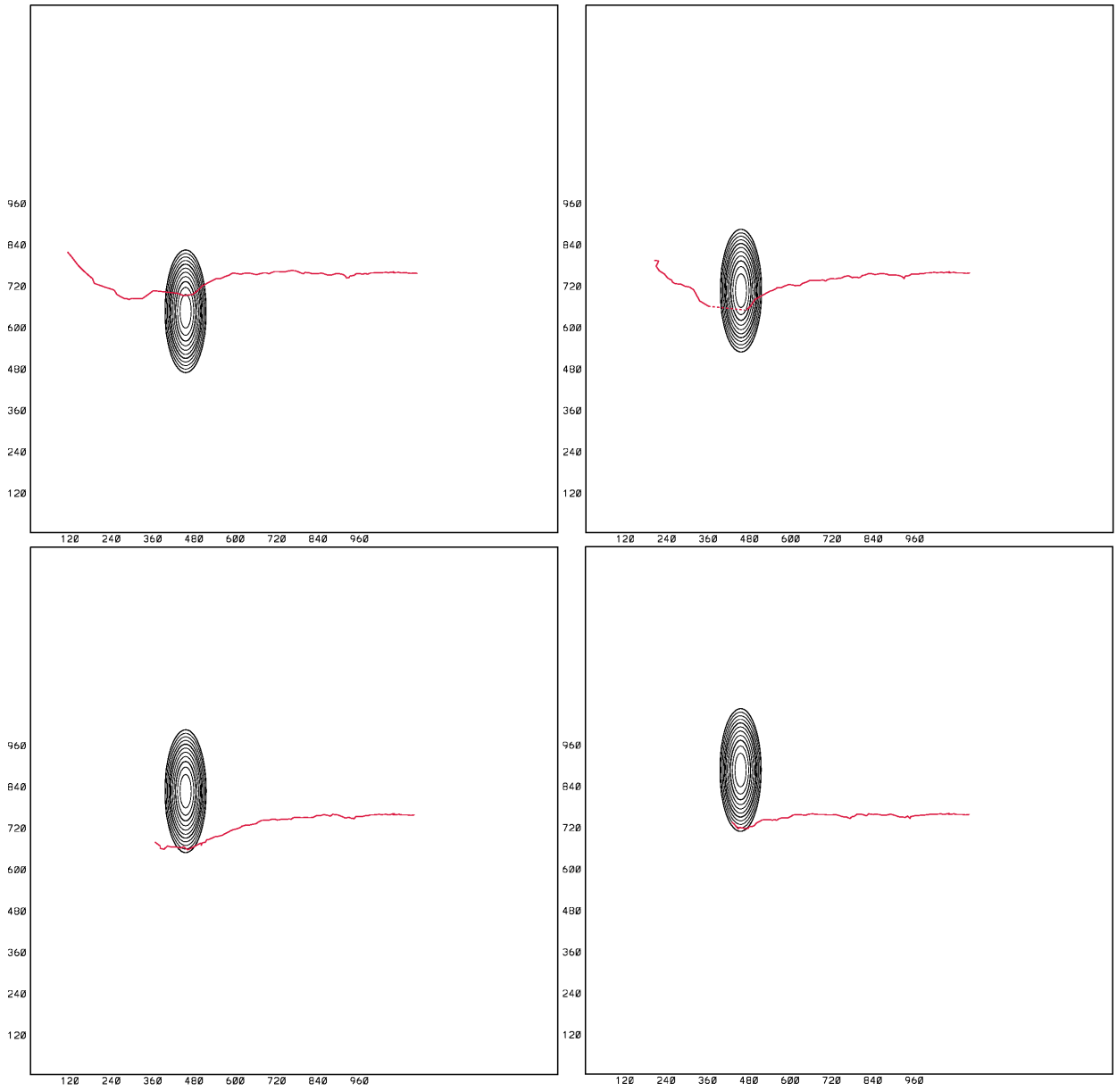

FIG. 7: Same as Fig. 5 for y=20 (ul), y=10 (ur), y=-10 (bl), and y=-20 (br) simulations.

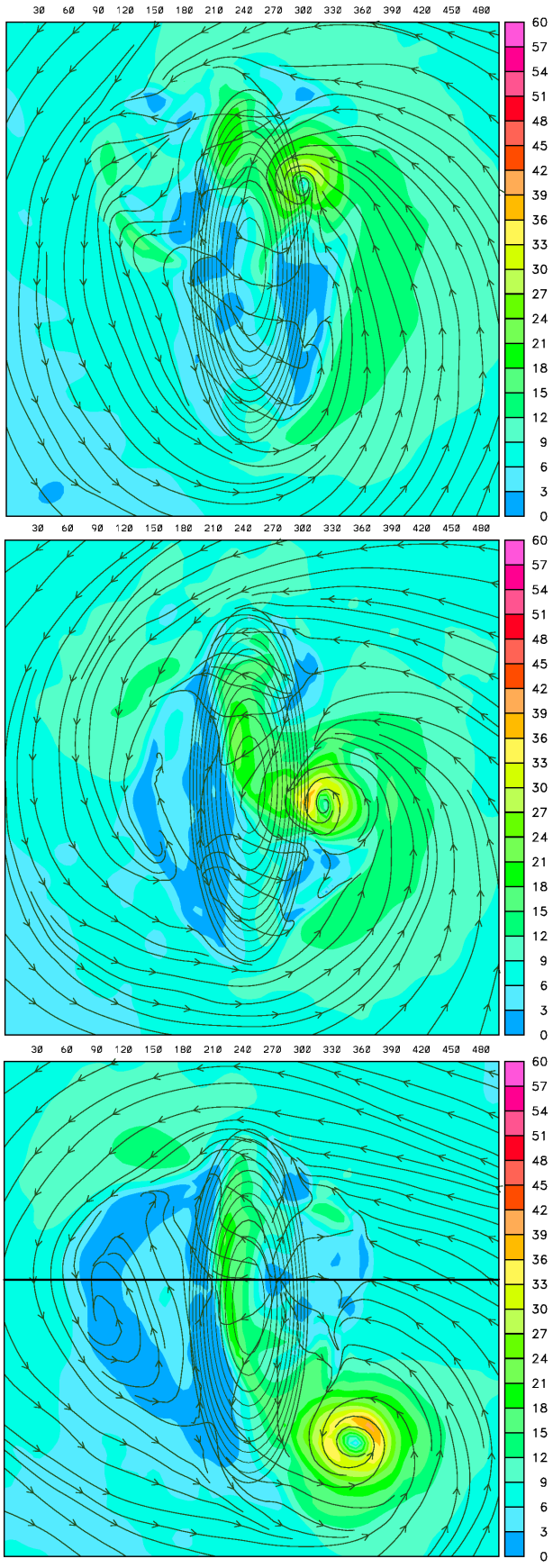

FIG. 8: Same as Fig. 3 for a landfall on the south end of the island.

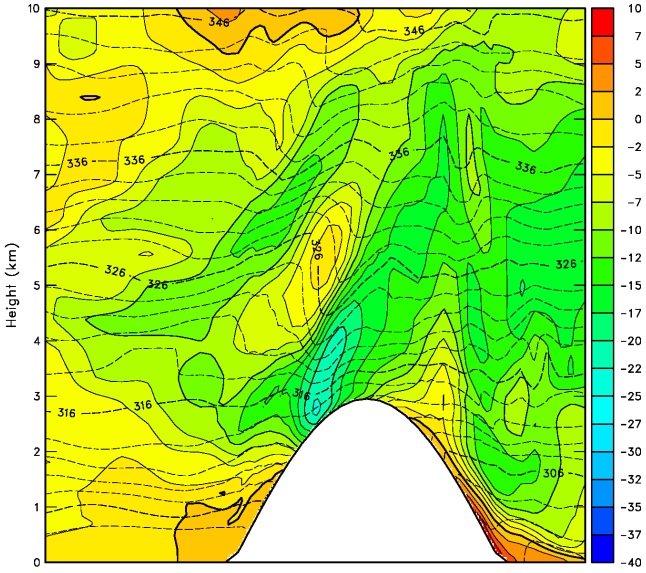

FIG. 9: Zonal wind speed (shaded) and isentropes (dashed lines) through the cross-section shown in Fig. 8 (bottom).

for southern landfall events. These areas represent an additional challenge to forecasting wind damage in association with a landfalling typhoon.

Obviously, there are still a very large number of control parameters which can still be explored, including storm intensity, island orientation (as a proxy for varying storm tracks), and mean flow speed. These studies may help to determine whether a particular leeside location will be sheltered from higher wind speeds or experience a downslope windstorm in excess of what would be produced by the typhoon itself. Finally, the precipitation distribution resulting from both the flow structure and the pre-existing convection needs further attention.

ACKNOWLEDGMENTS

The authors would like to thank Dr. Richard Hodur who helped to develop the early versions of the idealized tropical cyclone code. This research was funded by the National Research Council and Office of Naval Research Program Element 0602435N.

REFERENCES

Clark, T. L., and W. R. Peltier, 1977: On the evolution and stability of finite-amplitude mountain waves. *J. Atmos. Sci.,* **34,** 1715-1730.

Dunion, J. P., and C. S. Marron, 2008: A reexamination of the Jordan mean tropical sounding based on awareness of the Saharan air layer: Results from 2002. *J. Climate,* **21,** 5242-5253.

Fudeyasu, H., T. Kuwagata, Y. Ohashi, S. Suzuki, Y. Kiyohara, and Y. Hozumi, 2008: Numerical study of the

local downslope wind “Hirodo-Kaze” in Japan. *Mon. Wea. Rev.,* **136,** 27-40.

Lin, Y.-L., S.-Y. Chen, C. M. Hill, and C.-Y. Huang, 2005: Control parameters for the influence of a mesoscale mountain range on cyclone track continuity and deflection. *J. Atmos. Sci.,* **62,** 1849-1866.

Ramsay, H. A., and L. M. Leslie, 2008: The effects of complex terrain on severe landfalling Tropical Cyclone Larry (2006) over northeast Australia. *Mon. Wea. Rev.,* **136,** 4334-4354.

Reynolds, C. A., J. D. Doyle, R. M. Hodur, and H. Jin, 2010: Naval Research Laboratory multi-scale targeting guidance for T-PARC and TCS-08. In press.

Smolarkiewicz, P. K., and R. Rotunno, 1989: Low Froude number flow past three-dimensional obstacles. Part I: Baroclinically generated lee vortices. *J. Atmos. Sci.,* **46,** 1154-1164.

Wu, C.-C., and Y.-H. Kuo, 1999: Typhoons affecting Taiwan: Current understanding and future challenges. *Bull. Amer. Meteor. Soc.,* **80,** 67-80.

Yeh, T.-C., and R. L. Elsberry, 1993a: Interaction of typhoons with the Taiwan orography. Part I: Upstream track deflections. *Mon. Wea. Rev.,* **121,** 3193-3212.

——-, and ——-, 1993b: Interaction of typhoons with the Taiwan orography. Part II: Continuous and discontinuous tracks across the island. *Mon. Wea. Rev.,* **121,** 3213-3233.